



Harding, T., Rames, C., Teh, H. Y., Mill, T., Na, J., Chen, A., & Herrmann, G. (2017). Engine torque estimation with integrated unknown input observer and adaptive parameter estimator. In *Proceedings of the 20th IFAC World Congress* (Vol. 50, pp. 11058-11063). (IFAC-PapersOnLine).
<https://doi.org/10.1016/j.ifacol.2017.08.2487>

Peer reviewed version

Link to published version (if available):
[10.1016/j.ifacol.2017.08.2487](https://doi.org/10.1016/j.ifacol.2017.08.2487)

[Link to publication record in Explore Bristol Research](#)
PDF-document

This is the author accepted manuscript (AAM). The final published version (version of record) is available online via Elsevier. Please refer to any applicable terms of use of the publisher.

University of Bristol - Explore Bristol Research

General rights

This document is made available in accordance with publisher policies. Please cite only the published version using the reference above. Full terms of use are available:
<http://www.bristol.ac.uk/pure/about/ebr-terms>

Engine Torque Estimation with Integrated Unknown Input Observer and Adaptive Parameter Estimator

Thomas Harding*, Clement Rames*, Huang Yu Teh*, Toby Mill*, Jing Na* #, Anthony Chen*, Guido Herrmann*

* Department of Mechanical Engineering, University of Bristol, BS8 1TR, UK.

Faculty of Mechanical & Electrical Engineering, Kunming University of Science & Technology, Kunming, 650500 China
(e-mail: najing25@163.com; g.herrmann@bristol.ac.uk)

Abstract: This paper presents an integrated estimation scheme for the effective engine torque in automotive systems. This leads to a cascaded estimation structure, composed of an adaptive parameter estimator for the augmented wheel dynamics and the longitudinal motion, and an unknown input observer for the engine crankshaft dynamics. The adaptive parameter estimator has the ability to track time-varying parameters and can therefore provide an estimate of the driving torque for the wheels. Then this estimated torque is transmitted to the engine as the load torque through the drivetrain, and is used to design the unknown input observer. The standard models of driveline and tyre friction are modified for ease of parameter estimation. Only the engine crankshaft velocity, the wheel rotational velocity, and the vehicle longitudinal speed are needed. The convergence of these estimators is analyzed. Simulations based on a dynamic simulator built with commercial vehicular simulation software, IPG CarMaker, and Matlab/Simulink show promising results.

Keywords: Engine torque estimation, automotive powertrain, tyre friction, unknown input observer.

1. INTRODUCTION

Engine torque is an important variable in many automotive applications, e.g. powertrain control (Kiencke & Nielsen, 2000) and in-car parameters estimation (Mahyuddin, Na, Herrmann, Ren, & Barber, 2014). However, torque transducers are very expensive making them unsuitable for use in production vehicles. Thus, it is necessary to estimate the unknown engine torque based on available variables (Helm, Kozek, & Jakubek, 2012; Hong, Shen, Ouyang, & Kako, 2011; Wang, Krishnaswami, & Rizzoni, 1997). With accurate engine models, several estimation techniques have been proposed for automotive applications, e.g. Kim et al. (Kim, Rizzoni, & Utkin, 1998) have used a mean value engine model (MVEM) (Crossley & Cook, 1991; Hendricks & Sorenson, 1990) to develop several estimation schemes.

To address the engine torque estimation, Falcone et al. (Falcone, Fiengo, & Glielmo, 2005) designed a Linear Quadratic (LQ) ‘controller’ to estimate engine torque. Stotsky (Stotsky & Kolmanovsky, 2002) compared three unknown input observers for air charge estimation, and also showcased the potential of chaining multiple estimators together to enable simultaneous estimation of the throttle air mass flow, manifold pressure, and the port air mass flow. Hong et al. (Hong, et al., 2011) presented model-based torque observer configurations depending on available sensors. Kalman filters have also been used (Helm, et al., 2012). Recently, we introduced two novel engine torque estimation strategies (Na, Herrmann, Burke, & Brace, 2015): unknown input observer and adaptive parameter estimation. This unknown input observer has a very simple structure and is easy to be implemented. The new adaptive laws driven by the parameter estimation error (Na, Mahyuddin, Herrmann, Ren, & Barber, 2015) can achieve fast convergence even for time-varying parameters. However, in these estimation methods, it is assumed that the load torque applied to the engine should be available or precisely measured.

It is known that the load torque acting on the engine is indeed the driving torque for the drivetrain (Chen & Gao, 2013). Thus, one can further investigate the estimation of engine torque throughout the powertrain. However, one critical difficulty is the determination of the tyre-road friction (Kiencke & Nielsen, 2000). For this purpose, Pacejka’s magic model (Pacejka, 2005) has been widely used in tyre friction estimation schemes, e.g. sliding mode observer (Patel, Edwards, & Spurgeon, 2010), slip-slope friction coefficient identification (Hong, Erdogan, Hedrick, & Borrelli, 2013; Muller, Uchanski, & Hedrick, 2003; Rajamani, Phanomchoeng, Piyabongkarn, & Lew, 2012). However, some essential parameters in the Pacejka model should be determined a priori, which is not a trivial task. It is also noted that the integration of engine torque estimators with friction estimation has been rarely reported.

The aim of this paper is to present an integrated estimation methodology, which is suited to estimate the effective engine torque from velocity data across the drivetrain. This can be achieved by applying a recently proposed unknown input observer (Na, Herrmann, et al., 2015) for the engine rotation dynamics, and an improved adaptive parameter estimator for the augmented wheel and longitudinal dynamics. The latter one provides an estimate of the torque transmitted from the drivetrain, which can be taken as the load torque applied to the engine. Then the effective engine torque can be taken as an ‘unknown input’ for the engine dynamics, and thus can be estimated via an unknown input observer (Na, Herrmann, et al., 2015) with this estimated load torque and the measured crankshaft velocity. This leads to a cascaded estimation framework, where only the engine crankshaft velocity, wheel rotational velocity and the vehicle longitudinal speed are used. A dynamic simulator using the commercial software IPG CarMaker and Matlab is built to verify the proposed methods.

2. MODELLING OF AUTOMOTIVE POWERTRAIN

This section outlines the major components in the vehicle

powertrain systems: engine, drivetrain and wheels. The engine acts as a torque source for the crankshaft. The longitudinal forces from the car body are transmitted to the powertrain, and taken as a torque load acting on the engine.

2.1 Engine Model

To model the engine dynamics, a mean value engine model (MVEM) (Crossley & Cook, 1991) (Hendricks & Sorenson, 1990) has been proposed with satisfactory modelling accuracy. The main focus of this paper is on the estimation of effective engine torque, hence, we will only present the rotational dynamics of the crankshaft.

$$J_e \dot{\omega}_{cs} = T_{ind} - T_{fric} - T_{pump} - T_{load} = T_{Eng} - T_{load} \quad (1)$$

where J_e is the moment of inertia, ω_{cs} is the crankshaft velocity, T_{fric} , T_{pump} , T_{load} are the frictional loss, pumping loss and the load, respectively, T_{ind} is the indicated torque from the combustion. The load torque T_{load} applied on the engine comes from the wheels. The objective is to estimate the effective torque $T_{Eng} = T_{ind} - T_{fric} - T_{pump}$ by using the measured engine and vehicle variables.

Remark 1: In our previous work (Na, Herrmann, et al., 2015), we have estimated T_{Eng} by presenting a new unknown input observer based on (1). However, in that work we assume that the load torque T_{load} is precisely known or measured. The current work will further remove this assumption, where an estimate of T_{load} can be obtained via an adaptive parameter estimator by considering the powertrain dynamics.

2.2 Drivetrain Model

The realistic drivetrain consists of a set of components (Kiencke & Nielsen, 2000): crankshaft with flywheel, clutch, transmission (gearbox controlled by shift logic), final drive and driveshaft. In order to present efficient models, one may only consider the most significant physical characteristics of the drivetrain. In this case, the simplest drivetrain function would be to assume no compliance or power losses, but to account for gearing by dividing the combined gear ratio

$$T_{Trans} = T_{Drive} / (I_t \times I_f) \quad (2)$$

where T_{Trans} is the load torque acting on the crankshaft (If the clutch in the drivetrain is engaged, we know $T_{load} = T_{Trans}$ (Kiencke & Nielsen, 2000)), T_{Drive} is the driving torque acting on the wheels. I_t is the gear ratio of the transmission gear box, and I_f is the conversion ratio of the final drive.

The largest power loss in the drivetrain is indeed friction, followed by damping. Hence, a modified drivetrain model accounting for the lumped friction torque loss is given by

$$T_{Trans} = \frac{T_{Drive}}{I_t \times I_f} + T_{Loss} = \frac{T_{Drive}}{I_t \times I_f} + \omega_c \left(\frac{d_t}{I_t^2} + \frac{d_f}{I_f^2} \right) \quad (3)$$

where ω_c is the velocity of the clutch on the transmission side, and d_t , d_f are the damping constants for the transmission and final drive, T_{Loss} is the friction loss. The unknown velocity ω_c is on the transmission side of the clutch. Since the measured velocity that most closely resembles it is the wheel velocity ω_w (Kiencke & Nielsen, 2000), it is possible to get ω_c by multiplying ω_w by the gear ratio, i.e. $\omega_c = I_t I_f \omega_w$.

In the modified model (3), the friction loss is modelled as rotational damping. Although not entirely accurate due to the exclusion of coulomb forces, this simplified model was found to be a surprisingly accurate predictor of real world performance (Kiencke & Nielsen, 2000).

Remark 2: In the drivetrain model in this paper, the clutch is assumed to be constantly engaged and acts as a rigid shaft. By comparison of the velocity and torque outputs, we found that the drivetrain model captures the necessary powertrain dynamics. Moreover, the drivetrain in (3) with friction compensation can improve the overall estimation response.

2.3 Wheels Rotation and Longitudinal Motion

This set of vehicle components transfer the torque T_{Drive} to the wheel, which serves as the power source for the vehicle longitudinal motion. The tyre is a critical part as it provides the interface between the wheel rotation and the longitudinal motion. The torque from the drivetrain acts to move the tyre tread backwards relative to the road. This torque has been found to be a function of the slip (Rajamani, et al., 2012) between the tyre and road. The slip ratio S_x is given by

$$S_x = (r_e \omega_w - V) / V \quad (4)$$

where r_e is the radius of the wheels, ω_w is the wheel rotation velocity, and V is the vehicle longitudinal speed.

One of the most commonly used empirical models for the friction force is Pacejka's Formula (Pacejka, 2005)

$$\frac{F_x}{F_z} = D \sin(C \arctan[BS_x - E(BS_x - \arctan(BS_x))]) \quad (5)$$

where F_z is the normal tyre force, and F_x is the frictional force in the longitudinal direction. The curve of (5) depends on the parameters B to E , which are related to the road conditions and tyre materials. One difficulty for applying Pacejka's model (5) is to determine its parameters (Rajamani, et al., 2012), which are not linearly parameterized.

It is known that the parameter estimation techniques require that the parameters to be estimated are linearly parameterized. For this reason, a modified tyre-road friction model is proposed in this paper

$$\frac{F_x}{F_z} = a_1 \tanh(a_2 S_x) - a_7 \tanh(a_3 S_x) + a_4 \tanh(a_5 S_x) + a_6 S_x \quad (6)$$

where the tyre model parameters a_1, a_4, a_6, a_7 can be online estimated, and a_2, a_3, a_5 can be set based on experimental data. An obvious weakness here is that this set of parameters may be a function of the changing driving environment, a further simplified linear friction model is also used

$$\frac{F_x}{F_z} = a_1 S_x \quad (7)$$

where a_1 is the linearized 'stiffness' of the tyre with respect to the slip ratio only. This model has the advantage that no parameters must be set, but the disadvantage that it may fail to capture the nonlinearities at very high slip ratios. These two friction models are tested and compared in simulations.

The majority of recreational cars are front-wheel driven; this will cause a larger slip for a given torque magnitude than rear wheels. Thus, a possible simplification would be to assume that all torques are transmitted through the front wheels, i.e. the wheel dynamics can be described by

$$J_w \dot{\omega}_w = \frac{T_{Drive}}{2} - r_e F_x \quad (8)$$

where J_w is the moment of inertia of a single wheel, T_{Drive} is the torque transmitted from the drivetrain in (2) or (3), F_x is the friction force in (6) or (7).

To facilitate the estimation, the car can be considered a single lumped mass propelled forward by F_x from each front wheel. The resistant aerodynamic drag is more significant than the rolling resistance. Hence, the longitudinal motion is described by

$$m\dot{V} = 2F_x - \rho AC_d V^2 \quad (9)$$

where m is the vehicle mass, V is the longitudinal speed, ρ , A , C_d are the air density, frontal area and the drag coefficient.

The aim for considering the wheel rotation (8) and longitudinal motion (9) is to estimate the driving torque T_{Drive} based on ω_w and V . Hence, we define the augmented state as $X = [V, \omega_w]^T$, and obtain an augmented system as

$$\dot{X} = \begin{bmatrix} \dot{V} \\ \dot{\omega}_w \end{bmatrix} = \begin{bmatrix} 2/m \\ -r_e/J_w \end{bmatrix} F_x + \begin{bmatrix} 0 \\ 1/2J_w \end{bmatrix} T_{Drive} + \begin{bmatrix} -1/m \\ 0 \end{bmatrix} F_{drag} \quad (10)$$

where $F_{drag} = \rho AC_d V^2$ is the aerodynamic drag force.

3. TORQUE ESTIMATION SCHEME

In this section, we will present an integrated estimation scheme to obtain the effective engine torque T_{Eng} . For this purpose, a cascaded estimation structure (Fig.1) will be suggested, which consists of an adaptive parameter estimator based on (10) and an unknown input observer based on (1).

In this scheme, the adaptive parameter estimator can provide an estimate of the driving torque T_{Drive} , which will be traced back through the drivetrain to arrive at an estimate of T_{Trans} . The estimate of T_{Trans} is then used in the unknown input observer to get the estimate of T_{Eng} . The variables that should be measured via sensors are the engine crankshaft velocity ω_{cs} , the wheel rotational velocity ω_w and the vehicle longitudinal speed V .

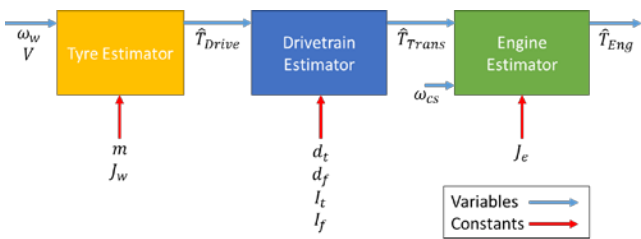


Fig. 1 Estimator integration scheme.

3.1 Adaptive Parameter Estimator

The aim of this estimator is to estimate the driving torque T_{Drive} using ω_w and V . For this purpose, we take T_{Drive} as a time-varying parameter in (10), and then present an adaptive law with guaranteed convergence for estimating such time-varying parameters. Here, F_x in (10) is also unknown. Thus, the dynamics of (10) are rewritten in two different alternative forms for adaptive parameter estimation approaches. To this end, we substitute (6) and (7) into (10) such that

$$\dot{X} = \underbrace{\frac{2F_z}{m} \begin{bmatrix} \tanh(a_2 S_x) & -\tanh(a_3 S_x) & \tanh(a_5 S_x) & S_x & \frac{-1}{m} & 0 \\ 0 & 0 & 0 & 0 & 0 & \frac{1}{2J_w} \end{bmatrix}}_{\Phi} \underbrace{\begin{bmatrix} a_1 \\ a_7 \\ a_4 \\ a_6 \\ \frac{m}{2F_z} F_{drag} \\ \frac{m}{2F_z} T_{Drive} \end{bmatrix}}_{\Theta} + \underbrace{\begin{bmatrix} 0 \\ -r_e/J_w \end{bmatrix}}_{\Psi} \hat{F}_x \quad (11)$$

or

$$\dot{X} = \underbrace{\frac{2F_z}{m} \begin{bmatrix} S_x & -1/m & 0 \\ 0 & 0 & 1/2J_w \end{bmatrix}}_{\Phi} \underbrace{\begin{bmatrix} a_1 \\ (m/2F_z) F_{drag} \\ (m/2F_z) T_{Drive} \end{bmatrix}}_{\Theta} + \underbrace{\begin{bmatrix} 0 \\ -r_e/J_w \end{bmatrix}}_{\Psi} \hat{F}_x \quad (12)$$

In the following developments, the estimators based on equations (11) and (12) are referred to as the *Trigonometric Estimator* and *Linear Estimator*, respectively, referring to the nature of the parameterization of F_x given in (6) or (7).

In (11) and (12), we separate F_x into its constituent parts. This is done only for the top line of the state vector, while the estimated \hat{F}_x is used at the bottom line based on the estimated parameters, i.e. $\hat{F}_x = F_z \hat{a}_1 S_x$ for (12) and $\hat{F}_x = F_z [\hat{a}_1 \tanh(a_2 S_x) - \hat{a}_7 \tanh(a_3 S_x) + \hat{a}_4 \tanh(a_5 S_x) + \hat{a}_6 S_x]$ for (11). This approach avoids introducing terms that are a multiple of each other, i.e. these may cause loss of rank of Φ . Hence, this idea can help to fulfil the persistent excitation (PE) condition (Na, Mahyuddin, et al., 2015) imposed on Φ for ensuring the convergence of adaptive laws.

To simplify the following analysis, we can represent (11) and (12) in a unified form

$$\dot{X} = \Phi \Theta + \Psi \quad (13)$$

Remark 3: Most of standard parameter estimation methods are only suited for constant parameters (Ioannou & Sun, 1996). In our case, the unknown parameter Θ in (13) involves time-varying dynamics T_{Drive} and F_{drag} . Thus, we will further extend our previous adaptation algorithm (Na, Mahyuddin, et al., 2015) to improve the estimation response.

For derivation of the estimation scheme, the measured dynamics are low-pass filtered as

$$\begin{cases} k\dot{X}_f + X_f = X, & X_f(0) = 0 \\ k\dot{\Phi}_f + \Phi_f = \Phi, & \Phi_f(0) = 0 \\ k\dot{\Psi}_f + \Psi_f = \Psi, & \Psi_f(0) = 0 \end{cases} \quad (14)$$

Then, $\dot{X}_f = (X - X_f)/k$ can be verified. If k is very small then the cut-off frequency $1/k$ of the low-pass filter in (14) is very high, so that \dot{X}_f is virtually \dot{X} .

An auxiliary regression matrix P and vector Q can then be introduced as in (Na, Mahyuddin, et al., 2015)

$$\begin{cases} \dot{P} = -\beta P + \Phi_f^T \Phi_f, & P(0) = 0 \\ \dot{Q} = -\beta Q + \Phi_f^T \left[\frac{X - X_f}{k} - \Psi_f \right], & Q(0) = 0 \end{cases} \quad (15)$$

where $\beta > 0$ is a forgetting factor used to guarantee the boundedness of P and Q .

Then, we can derive auxiliary vectors W_1 and W_2 based on

P, Q and $X, X_f, \Psi_f, \Phi_f, \Psi_f$ as

$$W_1 = P\hat{\Theta} - Q \quad (16)$$

$$W_2 = \Phi_f^T \Phi_f \hat{\Theta} - \Phi_f^T [(X - X_f)/k - \Psi_f] \quad (17)$$

where $\hat{\Theta}$ is the estimate of Θ , which is updated based on the following adaptive law

$$\dot{\hat{\Theta}} = -\Gamma(W_1 + \kappa W_2) \quad (18)$$

where the learning gain Γ can be set as a constant diagonal matrix, and κ is an additional design parameter to balance faster tracking of varying parameters with unwanted noise. This additional term W_2 is crucial to allow fast tracking of time-varying parameters (Na, Herrmann, et al., 2015).

Before we present the convergence property of (18), we apply a low-pass filter $1/(ks+1)$ on both sides of (13) using the Swapping Lemma (Ioannou & Sun, 1996), such that

$$\dot{X}_f = \frac{X - X_f}{k} = \Psi_f + \Phi_f \Theta - \zeta \quad (19)$$

where $\zeta = L^{-1} \left[\frac{k}{ks+1} [\Phi_f \dot{\Theta}] \right]$ and the operator $L^{-1}[\bullet]$ is the inverse Laplace transform. It can be verified that $\|\zeta\| \leq \gamma$ for a positive constant γ due to that Φ_f and $\hat{\Theta}$ are bounded.

Then following a similar analysis as in (Na, Herrmann, et al., 2015), P can be considered as a filtered version of $\Phi_f^T \Phi_f$, Q is a filtered version of $\Phi_f^T \Phi_f \Theta - \Phi_f^T \zeta$. Then it follows

$$W_1 = -P\tilde{\Theta} + \psi \quad (20)$$

$$W_2 = -\Phi_f^T \Phi_f \tilde{\Theta} + \Phi_f^T \zeta \quad (21)$$

where $\psi = \int_0^t e^{-\ell(t-r)} \Phi_f^T(r) \zeta(r) dr$ is a bounded signal, and $\tilde{\Theta} = \Theta - \hat{\Theta}$ is the estimation error.

Proposition 1: If the derivative of the unknown parameter $\dot{\Theta}$ is bounded and the regressor matrix Φ is PE, then the estimation error $\tilde{\Theta}$ of (18) exponentially converges to a compact set around zero, whose size depends on the bound of the residual error ζ defining the variations of $\dot{\Theta}$.

Proof. Please refer to (Na, Herrmann, et al., 2015) for a similar proof.

From the estimated parameter $\hat{\Theta}$, one can obtain the estimated driving torque $\hat{T}_{Drive} = \hat{\Theta}_m / 2F_z$, which can be used to calculate the estimated torques \hat{T}_{Trans} and \hat{T}_{load} via (2) or (3).

Remark 4: The forgetting factor β in (15) defines the cut-off frequency of the filter $1/(s+\beta)$ in (15). Thus, a higher β can help to track faster changes in Θ , with the possible downside of transmitting much noise.

Remark 5: It is shown in (20)-(21) that the vectors used to drive the adaptive law (18) contains the estimation error $\tilde{\Theta}$. This is also particularly useful for estimating time-varying parameters. In case Θ is constant, i.e. $\dot{\Theta} = 0$, we can verify that $\zeta = \psi = 0$ from (19)-(21). In this case, exponential convergence of $\tilde{\Theta}$ to zero can be proved.

3.2 Unknown Input Observer

In Section 3.1, we have obtained the estimated \hat{T}_{load} based

on \hat{T}_{Drive} and hence \hat{T}_{Trans} . Thus, the unknown effective engine torque T_{Eng} can be taken as a virtual ‘unknown input’ in (1). In this case, the principle of an unknown input observer (Na, Herrmann, et al., 2015) can be used to estimate T_{Eng} using the estimate of T_{load} and the measured crankshaft velocity ω_{cs} .

Then, we define the filtered variables of ω_{cs} and \hat{T}_{load} as

$$\begin{cases} k\dot{\omega}_{cs,f} + \omega_{cs,f} = \omega_{cs}, & \omega_{cs,f}(0) = 0 \\ k\dot{T}_{load,f} + T_{load,f} = \hat{T}_{load}, & T_{load,f}(0) = 0 \end{cases} \quad (22)$$

where k is the filter parameter as used in (14).

Lemma 1: Consider the engine crankshaft dynamics in (1) and the filter operation in (22), then the variable

$E = J_e \frac{\omega_{cs} - \omega_{cs,f}}{k} + T_{load,f} - T_{Eng}$ is bounded for any finite $k > 0$, and decreases exponentially. Moreover, $\lim_{k \rightarrow 0} \lim_{t \rightarrow \infty} E = 0$

holds, such that $J_e \frac{\omega_{cs} - \omega_{cs,f}}{k} + T_{load,f} - T_{Eng} = 0$ is an invariant manifold for any $k > 0$.

Proof. We refer to (Na, Herrmann, et al., 2015) for a similar proof.

The above manifold provides a mapping from available variables $(\omega_{cs}, \omega_{cs,f}, T_{load,f})$ to the unknown torque T_{Eng} without knowing any information of the angular acceleration $\dot{\omega}_{cs}$. Thus, a feasible estimator of T_{Eng} is given

$$\hat{T}_{Eng} = J_e \frac{\omega_{cs} - \omega_{cs,f}}{k} + T_{load,f} \quad (23)$$

Then following a similar analysis as in (Na, Herrmann, et al., 2015), one can verify that $\hat{T}_{Eng} = T_{Eng}$. This means that the proposed estimate is equivalent to the filtered version of the unknown torque T_{Eng} , which is given by

$$k\dot{\hat{T}}_{Eng,f} + \hat{T}_{Eng,f} = T_{Eng}, \hat{T}_{Eng,f}(0) = 0 \quad (24)$$

Proposition 2: Consider the crankshaft dynamics (1) and the effective engine torque estimator (23). If the engine torque \dot{T}_{Eng} is bounded, then the estimation error $\tilde{T}_{Eng} = T_{Eng} - \hat{T}_{Eng}$ can exponentially converge to a small compact set around zero, and $\hat{T}_{Eng} \rightarrow T_{Eng,f}$ holds for $k \rightarrow 0$ and $\dot{T}_{Eng} = 0$.

Proof: Please refer to (Na, Herrmann, et al., 2015) for details.

4. SIMULATIONS

4.1 Simulation scenarios

To show the validity of the proposed estimators in realistic vehicle driving scenarios, a commercial vehicle simulation package, IPG CarMaker, was chosen to provide data of wheel rotation and longitudinal motion dynamics with more realism than the simple model on which it is based. The default RealTime Tyre model embedded in CarMaker was used to demonstrate that the estimators can operate with inputs that do not conform exactly to the model given by Pacejka’s Magic Formula, and thus to validate their robustness. The RealTime Tyre model includes additional rolling resistance and a modified standstill model at speeds of less than 0.25m/s.

For torque estimation, IPG CarMaker does not offer the flexibility and transparency of a custom built model. Hence, a Simulink implementation, mixing custom built elements with

CarMaker provided dynamics, would be best suited for this application. Thus, in the constructed simulation system, the wheel and longitudinal vehicle dynamics from IPG CarMaker are incorporated with a bespoke MVEM model, speed control and a drivetrain model (Kiencke & Nielsen, 2000). In the drivetrain, the clutch and transmission logic were implemented in Stateflow, a Simulink package that allows an event driven control logic. Simulation parameters are listed in Table 1. The first column were the default values in CarMaker, while the second column were tuned manually to give the best possible results via a trial-and-error method. In IPG CarMaker, wheel speed sensors are present to calculate the slip assuming that the wheels all spin at the same speed.

In what follows, we will first test the individual estimators: the Trigonometric Estimator and Linear Estimator from Section 3.1 and the unknown input observer from Section 3.2 are discussed first, and then the results of the integrated estimator for the effective engine torque are presented.

Table 1 Simulation parameters in IPG CarMaker & Simulink

Parameter	Value	Parameter	Value
Car Mass m	1463	Tyre parameter a_2	1.1
Wheel radius r_e	0.293	Tyre parameter a_3	3
Wheel inertia J_w	1.2	Tyre parameter a_5	45
Air density ρ	1.205	Forgetting factor β	10
Drag coefficient C_d	0.2	Filter gain k	0.001
Car frontal area A	2	Aux. Input gain κ	7
Normal force F_z	3588		

4.2 Validation of adaptive parameter estimator

We first test the adaptive parameter estimators with the trigonometric estimator (11) and linear estimator (12). It is shown in Fig. 2 that the largest positive friction occurs when the car accelerates, and the interruptions are caused by gear changes, when the torque input falls. The largest estimation error of F_x is within the first 5s, when the estimated parameters are converging (Fig.4). After that transient, the estimators track the signal effectively with noticeable errors at the braking points only, because the ignored nonlinearities are significant at these force magnitudes. However, the errors are slightly smaller in the trigonometric estimator than for the linear estimator. This implies that the main source of the error lies elsewhere, i.e. the distribution of braking torque between all four wheels or the couplings between the lateral and longitudinal forces on the tyres.

Estimation of the driving torque T_{Drive} in Fig. 3 is similarly accurate, although the large error peaks are not present. There is however a ‘steady-state’ error at other times, which does not diminish with increased estimator gains. This might be caused by the lack of complete convergence of \hat{F}_x used in (11) and (12). The estimated parameters of both estimators converge to an initial value within 3s in Fig.4; there is a lack of excitation until the vehicle begins to accelerate at 1s. However, the estimation of F_{drag} is poor, particularly for the trigonometric estimator. Since it is not as important to the overall estimator for T_{Drive} or F_x , it was not particularly considered in the gain tuning process.

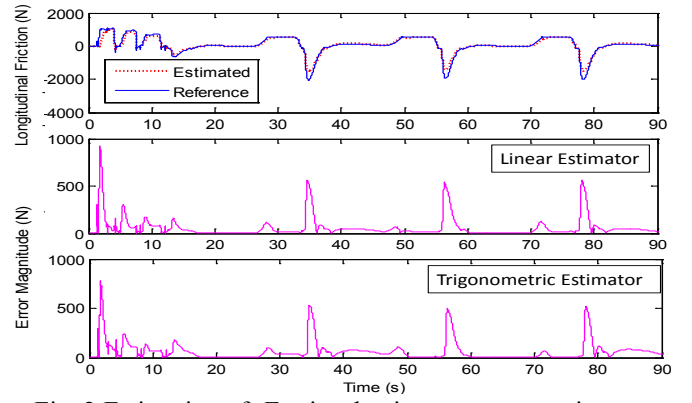


Fig. 2 Estimation of F_x via adaptive parameter estimator

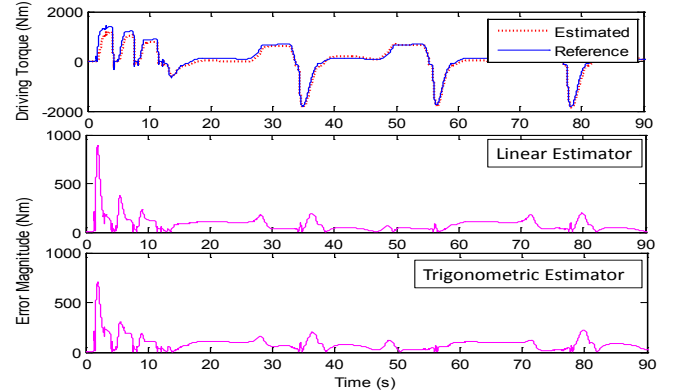


Fig. 3 Estimation of T_{Drive} via adaptive parameter estimator.

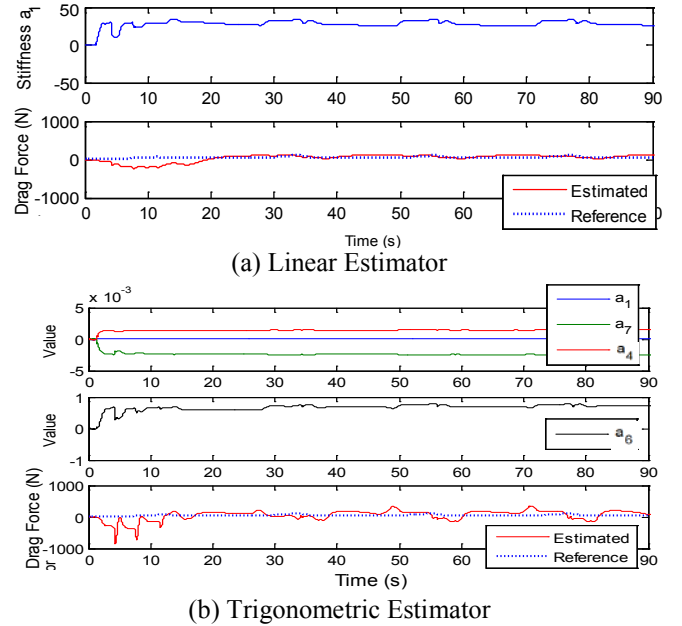


Fig. 4 Profiles of the estimated parameters

4.3 Validation of unknown input observer

The unknown input observer (23) is used to estimate T_{Eng} . In this simulation, the load torque T_{load} is known (this will be replaced by using \hat{T}_{Drive} in the integrated estimation later). Realistic driving conditions in IPG CarMaker is incorporated into a calibrated MVEM with the powertrain model, which contains fast accelerations and decelerations from 20 mph to 50 mph. A PID control was designed to emulate the driver's input for a demand square wave signal with a period of 30 s, oscillating between 9 and 22 m/s.

The proposed unknown input observer (UIO) is compared with a Sliding Mode Observer (SMO) and High Gain Observer (HGO) (Stotsky & Kolmanovsky, 2002). It is of interest to compare these three estimators during fast varying conditions, when the driver accelerates aggressively, or brakes suddenly. All three estimators, though completely different in nature, exhibit similar transient performance and steady state error in the absence of sensor noise (Fig.5).

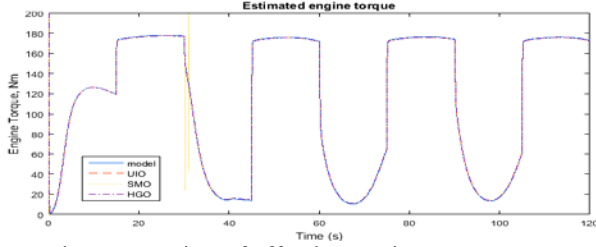
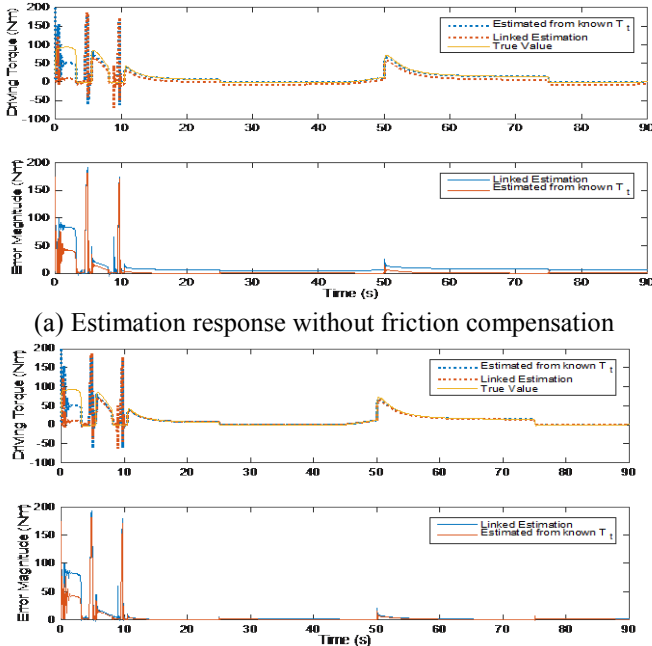


Fig.5 Estimation of effective engine torque T_{Eng} .

4.4 Integrated Estimation

In the final simulations, the adaptive parameter estimator (18) and the unknown input observer (23) are linked together to estimate the effective engine torque T_{Eng} . This integrated scheme is referred to as the linked estimator. For comparison, the case of known driving torque T_{Trans} (directly measured) is also tested, which is named as the unlinked estimator (Note in this case only the unknown input observer is needed).

It is shown in Fig. 6(a) that there is a significant transient error for the first 3s as the adaptive parameter estimator for \hat{T}_{Drive} needs a short period to achieve convergence (Fig. 3). Moreover, there is an error between the true value and the estimate in the 'steady-state', which may be due to the friction loss in the drivetrain. Then, we further change the drivetrain model as in (3) to account for the effect of the stiffness and damping in the drivetrain. One can find from Fig.6(b) that the linked estimator displays very similar performance to the unlinked estimator after convergence.



(b) Estimation response with friction compensation

Fig.6 Estimation of T_{Eng} via integrated estimation scheme.

5. CONCLUSIONS

This paper is concerned with the estimation of the effective engine torque. The powertrain dynamics from the engine to the vehicle wheels are considered. Then a cascade estimation scheme consisting of an adaptive parameter estimator and an unknown input observer is suggested. A modified tyre friction model and simplified drivetrain models are proposed to facilitate the parameter estimation. Only the measured engine crankshaft velocity, wheel rotation velocity and the vehicle longitudinal speed are used to implement the estimators. Extensive simulations with IPG CarMaker show that the proposed estimator method can cope well with fluctuations in realistic driving scenarios. For future practical applications, the requirement of the vehicle longitudinal speed should be further addressed.

Acknowledgment

This work was supported by the Marie Curie IEF Project AECE (grant FP7-PEOPLE-2013-IEF-625531) and National Natural Science Foundation of China (grant 61573174).

REFERENCES

- Chen, H., & Gao, B. (2013). *Nonlinear estimation and control of automotive drivetrains*: Springer Science & Business Media.
- Crossley, P. R., & Cook, J. A. (1991). A nonlinear engine model for drivetrain system development. In *IEE International Conference on Control* (pp. 921-925). Edinburgh, UK.: IET.
- Falcone, P., Fiengo, G., & Glielmo, L. (2005). Nicely nonlinear engine torque estimator. In *16th IFAC World Congress* (pp. 218-223). Prague.
- Helm, S., Kozek, M., & Jakubek, S. (2012). Combustion torque estimation and misfire detection for calibration of combustion engines by parametric kalman filtering. *IEEE Transactions on Industrial Electronics*, 59, 4326-4337.
- Hendricks, E., & Sorenson, S. C. (1990). Mean value modelling of spark ignition engines. In: SAE Technical paper.
- Hong, M., Shen, T., Ouyang, M., & Kako, J. (2011). Torque observers design for spark ignition engines with different intake air measurement sensors. *IEEE Transactions on Control Systems Technology*, 19, 229-237.
- Hong, S., Erdogan, G., Hedrick, K., & Borrelli, F. (2013). Tyre-road friction coefficient estimation based on tyre sensors and lateral tyre deflection: modelling, simulations and experiments. *Vehicle System Dynamics*, 51, 627-647.
- Ioannou, P. A., & Sun, J. (1996). *Robust Adaptive Control*. New Jersey: Prentice Hall.
- Kiencke, U., & Nielsen, L. (2000). Automotive control systems: for engine, driveline, and vehicle. In: IOP Publishing.
- Kim, Y.-W., Rizzoni, G., & Utkin, V. (1998). Automotive engine diagnosis and control via nonlinear estimation. *IEEE Control Systems*, 18, 84-99.
- Mahyuddin, M. N., Na, J., Herrmann, G., Ren, X., & Barber, P. (2014). Adaptive observer-based parameter estimation with application to road gradient and vehicle mass estimation. *IEEE Transactions on Industrial Electronics*, 61, 2851-2863.
- Muller, S., Uchanski, M., & Hedrick, K. (2003). Estimation of the maximum tire-road friction coefficient. *Journal of dynamic systems, measurement, and control*, 125, 607-617.
- Na, J., Herrmann, G., Burke, R., & Brace, C. (2015). Adaptive input and parameter estimation with application to engine torque estimation. In *2015 54th IEEE Conference on Decision and Control (CDC)* (pp. 3687-3692).
- Na, J., Mahyuddin, M. N., Herrmann, G., Ren, X., & Barber, P. (2015). Robust adaptive finite-time parameter estimation and control for robotic systems. *International Journal of Robust and Nonlinear Control*, 25, 3045-3071.
- Pacejka, H. (2005). *Tire and vehicle dynamics*: Elsevier.
- Patel, N., Edwards, C., & Spurgeon, S. (2010). Comparative analysis of two non-linear observers for estimation of tyre/road contact in the presence of imperfect measurements. *IET control theory & applications*, 4, 1501-1510.
- Rajamani, R., Phanomchoeng, G., Piyabongkarn, D., & Lew, J. Y. (2012). Algorithms for real-time estimation of individual wheel tire-road friction coefficients. *IEEE/ASME Transactions on Mechatronics*, 17, 1183-1195.
- Stotsky, A., & Kolmanovsky, I. (2002). Application of input estimation techniques to charge estimation and control in automotive engines. *Control Engineering Practice*, 10, 1371-1383.
- Wang, Y. Y., Krishnaswami, V., & Rizzoni, G. (1997). Event-based estimation of indicated torque for IC engines using sliding-mode observers. *Control Engineering Practice*, 5, 1123-1129.